Architecture of a Charge-Transfer State Regulating Light Harvesting in a Plant Antenna Protein

Tae Kyu Ahn, *et al.*

Science **320**, 794 (2008);
DOI: 10.1126/science.1154800

liposomes that contained Z rings, we counted 44 indentations over a total length of 575 μm. These indentations almost always coincided with a bright Z ring. Indentations or constrictions were thus five times more frequent in tubular liposomes that contained Z rings than in those without Z rings.

If the Z rings are generating a constriction force in the liposomes, they are doing this without a motor molecule. What could be the mechanism of force generation? We have previously reported that FtsZ can switch from a straight protofilament in GTP to a highly curved conformation in guanosine diphosphate (*8*, *13*, *14*). This conformational change is a candidate for force generation by FtsZ alone. Li *et al*. (*4*) also suggested that individual protofilaments may be generating a constriction force on the membrane segments to which they are attached.

A notable feature of the reconstituted Z rings is their strong tendency to form perfect closed rings that are oriented perpendicular to the axis of the tube. These features are consistent with the generation of a constriction force. If a filament grew longitudinally while attached to the membrane, in the absence of any force it might assume a loose helical shape or even more irregular course. If it is generating a constriction force, it would tend toward a minimum diameter, which would be a ring perpendicular to the axis (*15*).

The images of Li *et al*. (*4*) show individual protofilaments with few contacts between them. This raises the possibility that the assembly of protofilaments to form the long, thin Z ring is not propagated by direct lateral contacts between FtsZ protofilaments. An alternative mechanism is that a protofilament, by inserting amphipathic helices and exerting a force on the membrane, may produce distortions of the membrane that favor the attachment of additional protofilaments near the ends. This assembly, which would favor the formation of closed rings, might also be a source of constriction force.

Because FtsA is an actin homolog and is known to form dimers or oligomers (*16*, *17*), we initially thought that FtsA self-association might play an essential role in Z ring assembly. However, our reconstitution shows that neither FtsA nor downstream division proteins are required for Z ring assembly. FtsZ, a membrane tether, and the interior curved surface of a tubular liposome are sufficient for this assembly and the generation of a constriction force.

The earliest cellular life forms probably contained a replicating system of macromolecules surrounded by a lipid membrane. A mechanism would be needed to divide this living liposome. Our simple system may recapitulate the primordial division machine (*18*).

References and Notes

1. Y. Chen, H. P. Erickson, *J. Biol. Chem.* **280**, 22549 (2005).
2. S. Thanedar, W. Margolin, *Curr. Biol.* **14**, 1167 (2004).
3. P. C. Peters, M. D. Migocki, C. Thoni, E. J. Harry, *Mol. Microbiol.* **64**, 487 (2007).
4. Z. Li, M. J. Trimble, Y. V. Brun, G. J. Jensen, *EMBO J.* **22**, 4694 (2007).
5. D. E. Anderson, F. J. Gueiros-Filho, H. P. Erickson, *J. Bacteriol.* **186**, 5775 (2004).
6. S. Pichoff, J. Lutkenhaus, *Mol. Microbiol.* **55**, 1722 (2005).
7. S. Pichoff, J. Lutkenhaus, *EMBO J.* **21**, 685 (2002).
8. H. P. Erickson, *Trends Cell Biol.* **7**, 362 (1997).
9. K. Dai, J. Lutkenhaus, *J. Bacteriol.* **173**, 3500 (1991).
10. S. D. Redick, J. Stricker, G. Briscoe, H. P. Erickson, *J. Bacteriol.* **187**, 2727 (2005).
11. Methods are available as supporting material on *Science* Online.
12. L. Romberg, M. Simon, H. P. Erickson, *J. Biol. Chem.* **276**, 11743 (2001).
13. H. P. Erickson, D. W. Taylor, K. A. Taylor, D. Bramhill, *Proc. Natl. Acad. Sci. U.S.A.* **93**, 519 (1996).
14. C. Lu, M. Reedy, H. P. Erickson, *J. Bacteriol.* **182**, 164 (2000).
15. S. S. Andrews, A. P. Arkin, *Biophys. J.* **93**, 1872 (2007).
16. A. Feucht, I. Lucet, M. D. Yudkin, J. Errington, *Mol. Microbiol.* **40**, 115 (2001).
17. B. Lara *et al*., *Mol. Microbiol.* **55**, 699 (2005).
18. H. P. Erickson, *Bioessays* **29**, 668 (2007).

19. This work was supported by NIH grant GM66014.

Supporting Online Material

www.sciencemag.org/cgi/content/full/1154520/DC1
Materials and Methods
Fig. S1
References
Movies S1 to S3

21 December 2007; accepted 25 February 2008
Published online 17 April 2008;
10.1126/science.1154520
Include this information when citing this paper.

Architecture of a Charge-Transfer State Regulating Light Harvesting in a Plant Antenna Protein

Tae Kyu Ahn,[1,2]* Thomas J. Avenson,[2,3]* Matteo Ballottari,[4] Yuan-Chung Cheng,[2] Krishna K. Niyogi,[1,3] Roberto Bassi,[4]† Graham R. Fleming[1,2]†

Energy-dependent quenching of excess absorbed light energy (qE) is a vital mechanism for regulating photosynthetic light harvesting in higher plants. All of the physiological characteristics of qE have been positively correlated with charge transfer between coupled chlorophyll and zeaxanthin molecules in the light-harvesting antenna of photosystem II (PSII). We found evidence for charge-transfer quenching in all three of the individual minor antenna complexes of PSII (CP29, CP26, and CP24), and we conclude that charge-transfer quenching in CP29 involves a delocalized state of an excitonically coupled chlorophyll dimer. We propose that reversible conformational changes in CP29 can "tune" the electronic coupling between the chlorophylls in this dimer, thereby modulating the energy of the chlorophyll-zeaxanthin charge-transfer state and switching on and off the charge-transfer quenching during qE.

The photosynthetic apparatus in higher plants is designed to perform two seemingly opposing tasks: to efficiently harvest sunlight and transfer excitation energy to the reaction center (RC), but also to rapidly dissipate excessively absorbed light energy harmlessly as heat to avoid deleterious photodamage. Because highly reactive chemical species are inevitable by-products of photosynthesis, various regulatory processes are critical for the robustness of photosynthesis and for plant survival (*1*). Regulation of light harvesting is predominantly mediated by energy-dependent quenching (qE) (*2*, *3*), a phenomenon that depends on the transthylakoid pH gradient (ΔpH) (*4*), zeaxanthin (Z) (*5*), and the photosystem II (PSII) antenna-associated protein PsbS (*6*). However, precisely how and where within PSII these components interact to mediate qE at the molecular level is still not well understood. Identification of the precise molecular architecture that is responsible for this vital regulatory process could provide insight into the design principles of photoprotection in natural photosynthesis and could inspire approaches to engineer more robust artificial systems for solar energy conversion (*7*–*9*).

Two different mechanisms, which are not mutually exclusive, have been proposed recently to explain qE (*10*, *11*). According to Ruban *et al*. (*11*), qE occurs in the peripheral, trimeric antenna of PSII called LHCII (*12*), and its molecular mechanism involves energy transfer from chlorophyll a to a low-lying excited state of a carotenoid (lutein 1) in LHCII (*11*). A change in the conformation of a different carotenoid (neo-

[1]Physical Biosciences Division, Lawrence Berkeley National Laboratory, Berkeley, CA 94720, USA. [2]Department of Chemistry and QB3 Institute, University of California, Berkeley, CA 94720, USA. [3]Department of Plant and Microbial Biology, 111 Koshland Hall, University of California, Berkeley, CA 94720, USA. [4]Department of Science and Technology, University of Verona, 37134 Verona, Italy.

*These authors contributed equally to this work.
†To whom correspondence should be addressed. E-mail: grfleming@lbl.gov (G.R.F.); bassi@sci.univr.it (R.B.)

xanthin) was identified spectroscopically and correlated with LHCII quenching in vitro, and this conformational change was in turn correlated with qE in vivo (*11*). On the other hand, we have proposed a charge-transfer (CT) mechanism for qE on the basis of quantum chemical calculations (*13*) and ultrafast pump-probe experiments (*10*, *14*). The CT mechanism involves energy transfer from the chlorophylls bound to the PSII-LHCII supercomplex to a chlorophyll-Z heterodimer. The chlorophyll-Z heterodimer then undergoes charge separation followed by recombination, thereby transiently producing a Z radical cation ($Z^{\bullet+}$). Formation of $Z^{\bullet+}$ in thylakoids depends on the three components that are necessary for qE in vivo (*10*, *14*). In PSII, an inner layer of monomeric (minor) antenna proteins connects the peripheral LHCII trimers to the RC core complex (*15*, *16*). Evidence for CT quenching was recently demonstrated in a composite mixture of isolated minor antenna components (CP29, CP26, and CP24), whereas no trace of $Z^{\bullet+}$ formation signal could be found in isolated LHCII trimers (*14*). Thus, it is possible that different qE mechanisms are operating in different parts of the PSII antenna. Although each of these mechanisms has been proposed to account fully for qE (*11*, *14*), their relative contributions to qE in vivo remain to be determined.

To investigate the molecular architecture of CT quenching and to identify precisely which of the minor complexes are capable of mediating CT quenching, we carried out ultrafast transient absorption experiments in the spectral region of $Z^{\bullet+}$ absorption (*14*, *17*) using all three of the individual, isolated minor complexes. We expressed recombinant apoproteins of CP29, CP26, and CP24 in bacteria and reconstituted them in vitro with chlorophylls (a and b), lutein, and either Z or violaxanthin (V). In plants and isolated thylakoids, the reversible enzymatic conversion of V to Z is correlated with qE (*5*), and previous work has shown that CT quenching is associated with the presence of Z in intact systems (*10*) and in isolated proteins (*14*), whereas V-bound complexes are inactive. Herein we refer to the CP29 complexes reconstituted with Z and V as CP29-Z and CP29-V, respectively (table S1 and fig. S1). We excited the samples at 650 nm and probed the near-infrared (NIR) region where carotenoid radical cation species ($Car^{\bullet+}$) exhibited strong absorption (*10*, *14*).

Figure 1A shows the transient absorption profile for CP29-V as compared to that of CP29-Z. Both exhibit rapid rise components followed by exponential decays. However, relative to the CP29-V kinetics, the CP29-Z kinetic profile shows a larger initial amplitude rise, the component dynamics of which are clearly evident in the NIR transient absorption difference trace (Fig. 1A). For example, the difference profile is characterized by both very rapid (<500 fs) and slower (~5.5 ps) rise components, followed by single-exponential decay with a time constant of ~238 ps. Such a profile is indicative of transient $Car^{\bullet+}$ formation and is a signature of CT quenching (*10*, *14*). The spectrum reconstructed from a series of such difference profiles obtained by probing from 880 to 1080 nm exhibits a broad absorption band with a maximum at ~980 nm (Fig. 1B), in good agreement with the established $Z^{\bullet+}$ absorption characteristics (*10*, *14*). Similarly, the NIR transient absorption kinetics for CP26 and CP24 reconstituted with Z were also characterized by transient $Z^{\bullet+}$ formation. These combined results suggest that CT quenching (e.g., involving a chlorophyll-Z species that undergoes charge separation followed by recombination) occurs within all three minor complexes. This finding is consistent with the results of genetic and spectroscopic analyses showing that no single antenna protein is specifically required for qE (*14*, *18*–*20*).

To further explore the molecular details of CT quenching in CP29, we studied a series of mutant CP29 complexes that each lacked a specific chlorophyll. According to the previously reported homology structural model (*21*, *22*), CP29 contains eight chlorophyll-binding sites referred to as A1, A2, A3, A4, A5, B3, B5, and B6, along with two carotenoid-binding sites referred to as L1 and L2 (Fig. 2). Versions of CP29 with mutated ligands to each chlorophyll were reconstituted in vitro with chlorophylls (a and b), lutein, and either V or Z, and stable complexes each lacking specific chlorophylls were recovered except for the A1 mutant. These complexes are referred to as, for example, $CP29_{-A2}$, where the subscript denotes the missing chlorophyll (table S2 and figs. S2 to S5). Note that it has been established experimentally that Z binds specifically to the L2 domain; therefore, we can exclude the likelihood that chlorophyll A1 is directly involved in CT quenching (*23*, *24*).

The difference NIR transient absorption kinetic profile (blue trace) for $CP29_{-B3}$ is characterized by both rise and decay components that are signatures of $Z^{\bullet+}$ evolution during CT quenching (Fig. 3A), implying that CT quenching is active in the absence of chlorophyll B3. Likewise, the difference profiles for $CP29_{-A2}$, $CP29_{-A3}$, $CP29_{-A4}$, and $CP29_{-B6}$ also exhibit evidence of CT quenching irrespective of some variation in $Z^{\bullet+}$ signal that might derive from pleiotropic effects on protein structure (fig. S6). These data show that CT quenching in CP29 is not eliminated by the removal of chlorophylls A2, A3, A4, B3, or B6, thus excluding the likelihood of their participation in CT quenching. In contrast,

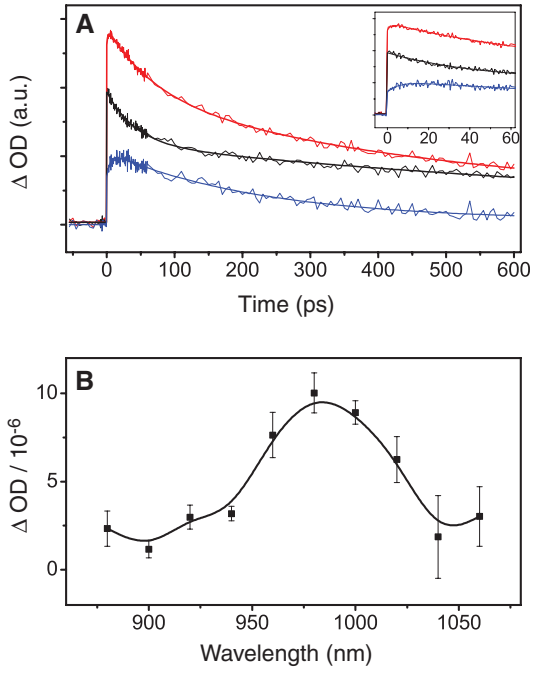

Fig. 1. NIR transient absorption kinetics for the CP29 minor complexes probed at 980 nm. (**A**) NIR transient absorption profiles for isolated CP29 complexes with excitation at 650 nm (chlorophyll b Q_y transition) and probing at 980 nm. The red and black profiles represent kinetics for CP29 complexes bound by Z and V, respectively. Note that the samples are prepared so that they have the same absorbance (0.3) at 650 nm, and these kinetic traces have not been normalized in any way. The difference kinetic trace (blue curve) is obtained by subtraction of the V-kinetic profiles from the Z-kinetic profiles. Inset: Transient absorption profiles over a shorter time region (0 to 60 ps). (**B**) NIR transient absorption spectrum for the isolated CP29 complexes. The spectrum was constructed from a series of NIR transient difference profiles obtained 15 ps after excitation by probing every 20 nm from 880 to 1080 nm. Error bars represent SE of five trials. The solid curve represents a b-spline interpolation among the experimental data points.

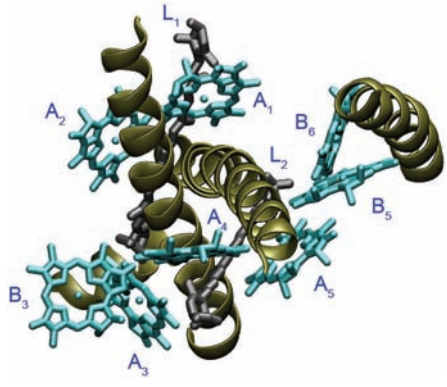

Fig. 2. CP29 homology structure model. The model shows eight chlorophylls and two carotenoid-binding sites (L1 and L2). The structure was constructed on the basis of homology data, mutational analyses, circular dichroism, and spectroscopic results (*21*, *22*). Chlorophylls A1 and A2 are located in the L1 carotenoid-binding pocket, whereas chlorophylls A4, A5, B5, and B6 are close to the L2 site.

the kinetic profiles for CP29$_{-A5}$, whether reconstituted with Z or V, are characterized solely by decay features attributable to chlorophyll excited-state absorption, and the transient absorption difference profile reveals no amplitude change relative to the noise level (Fig. 3B). The interpretation of this result is complicated by the fact that mutation of the amino acid residue that coordinates chlorophyll A5 also results in the loss of chlorophyll B5, specifically in Z-bound CP29 complexes (table S2). However, the kinetic profiles for CP29$_{-B5}$ (a complex lacking chlorophyll B5 only) are also characterized solely by chlorophyll excited-state absorption dynamics and no measurable $Z^{\bullet+}$ formation signal (Fig. 3C), which clearly indicates that CT quenching in CP29 involves chlorophyll B5. According to the homology structural model (Fig. 4), chlorophyll B5 is placed farther away from Z (~13 Å) than is chlorophyll A5 (~6 Å). The chlorophyll A5-B5 pair is positioned within the L2 domain and chlorophyll A5 is orientated roughly cofacial to, and centered along the axis of, the Z-binding site, which is in good agreement with the requirements for CT quenching previously predicted by quantum chemistry calculations (*13*). Furthermore, chlorophylls A5 and B5 are reported to be strongly coupled (*22*, *25*), and both are important for the regulation of chlorophyll excited states (*21*, *22*). Therefore, we conclude that CT quenching in CP29 most likely depends on both chlorophylls A5 and B5, and rather than a simple chlorophyll-Z heterodimer, the molecular site of CT quenching in CP29 comprises Z and a strongly coupled chlorophyll pair (A5 and B5).

What is the importance of this CT site architecture? Our finding indicates that the primary event of CT quenching in CP29 involves electron transfer from Z to a strongly coupled chlorophyll dimer in the A5-B5 pocket of CP29, rather than from Z to a monomeric chlorophyll molecule (*26*). Relative to a monomeric chlorophyll, a coupled chlorophyll dimer would be more favorable for CT quenching because the charge delocalization over the two chlorophylls will make the product CT state more stable. As a result, controlling the coupling strength between chlorophylls A5 and B5 in CP29, either by changing the distance between them or by altering their orientations, would modulate the reduction potential of the chlorophyll dimer and therefore could be used to switch on and off the CT quenching. This CT switching mechanism provides a potential molecular basis for the regulation of CT quenching during qE in the higher plant antenna.

The rapid reversibility of qE at the physiological level is thought to result from changes in the trans-thylakoid ΔpH that occur, for example, during fluctuations in incident solar flux density. It has been proposed that two thylakoid lumen-exposed glutamate residues of the PsbS protein sense these changes in pH (*27*) and induce protein conformational changes that control qE. Moreover, PsbS has recently been shown not to bind pigments (*28*) but to interact with CP29 (*29*). Therefore, we propose that pH-dependent protein conformational changes that are transduced from PsbS to CP29 (and possibly other minor antenna complexes) can alter the coupling strength between chlorophylls A5 and B5 in CP29 and induce CT quenching during qE. Experiments that can directly probe the efficiency of CT quenching while modulating the electronic coupling between chlorophylls A5 and B5 can test this proposal.

Converging results based on theoretical calculations, molecular genetic analysis, and ultrafast spectroscopy have shown that the mechanism involving CT quenching in minor complexes is emerging as a key component of qE. Our results show that CT quenching can occur in all three minor antenna complexes, which are positioned between LHCII and the RC, a perfect setting for regulating excitation energy transfer to the RC.

References and Notes

1. C. Külheim, J. Ågren, S. Jansson, *Science* **297**, 91 (2002).
2. P. Horton, A. V. Ruban, R. G. Walters, *Annu. Rev. Plant Phys.* **47**, 655 (1996).
3. K. K. Niyogi, *Annu. Rev. Plant Phys.* **50**, 333 (1999).
4. J. M. Briantais, C. Vernotte, M. Picaud, G. H. Krause, *Biochim. Biophys. Acta* **548**, 128 (1979).
5. B. Demmig-Adams, *Biochim. Biophys. Acta* **1020**, 1 (1990).
6. X.-P. Li *et al.*, *Nature* **403**, 391 (2000).
7. R. Berera *et al.*, *Proc. Natl. Acad. Sci. U.S.A.* **103**, 5343 (2006).
8. A. Hagfeldt, M. Gratzel, *Acc. Chem. Res.* **33**, 269 (2000).
9. T. A. Moore, A. L. Moore, D. Gust, *Philos. Trans. R. Soc. London Ser. B* **357**, 1481 (2002).
10. N. E. Holt *et al.*, *Science* **307**, 433 (2005).
11. A. V. Ruban *et al.*, *Nature* **450**, 575 (2007).
12. Z. Liu *et al.*, *Nature* **428**, 287 (2004).
13. A. Dreuw, G. R. Fleming, M. Head-Gordon, *Phys. Chem. Chem. Phys.* **5**, 3247 (2003).
14. T. J. Avenson *et al.*, *J. Biol. Chem.* **283**, 3550 (2008).
15. E. J. Boekema *et al.*, *Proc. Natl. Acad. Sci. U.S.A.* **92**, 175 (1995).
16. K. H. Rhee *et al.*, *Nature* **389**, 522 (1997).
17. S. Amarie *et al.*, *J. Phys. Chem. B* **111**, 3481 (2007).
18. J. Andersson, R. G. Walters, P. Horton, S. Jansson, *Plant Cell* **13**, 1193 (2001).
19. J. Andersson *et al.*, *Plant J.* **35**, 350 (2003).
20. L. Kovacs *et al.*, *Plant Cell* **18**, 3106 (2006).
21. R. Bassi, R. Croce, D. Cugini, D. Sandona, *Proc. Natl. Acad. Sci. U.S.A.* **96**, 10056 (1999).
22. G. Cinque, R. Croce, A. Holzwarth, R. Bassi, *Biophys. J.* **79**, 1706 (2000).

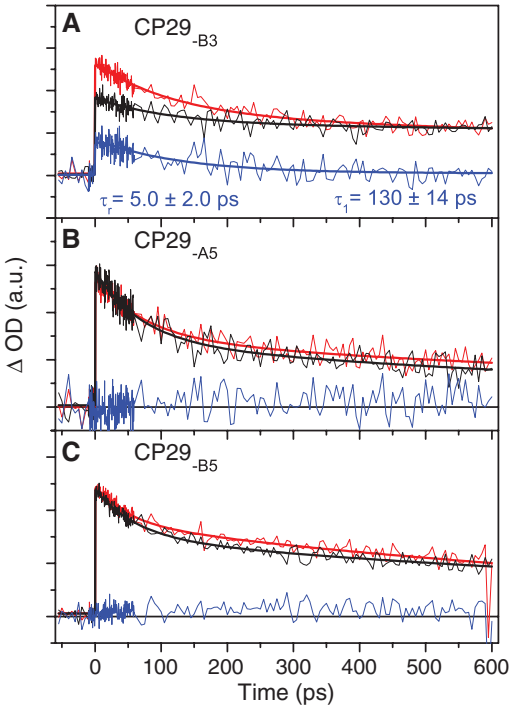

Fig. 3. NIR transient absorption kinetics for CP29 mutants lacking the ligands binding to chlorophylls B3, A5, and B5. Transient absorption profiles were measured using CP29$_{-B3}$ (**A**), CP29$_{-A5}$ (**B**), and CP29$_{-B5}$ (**C**). Other conditions are the same as Fig. 1A.

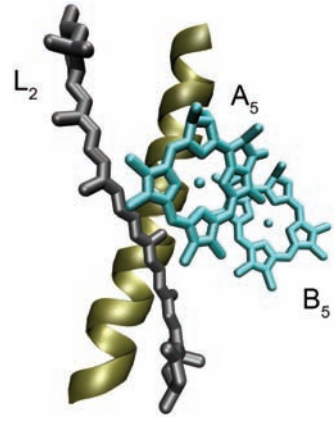

Fig. 4. Molecular details of the CT quenching site in CP29. Molecular sites responsible for CT quenching in CP29, including the Z bound in the L2 site and chlorophylls A5 and B5, are shown. On the basis of the homology model, the center-center distances for chlorophyll A5 to Z, chlorophyll A5 to chlorophyll B5, and chlorophyll B5 to Z are estimated to be ~6 Å, ~10 Å, and ~13 Å, respectively. The dihedral angle between chlorophylls A5 and B5 is about 41°. The structure indicates that chlorophylls A5 and B5 are strongly coupled to each other.

23. J. P. Connelly *et al.*, *Biochemistry* **36**, 281 (1997).
24. T. Morosinotto, S. Caffarri, L. Dall'Osto, R. Bassi, *Physiol. Plant.* **119**, 347 (2003).
25. H. van Amerongen, R. van Grondelle, *J. Phys. Chem. B* **105**, 604 (2001).
26. Formation of a delocalized chlorophyll dimer would depend on occupancy of both A5 and B5 sites by chlorophyll a. Although the A5 site exclusively binds chlorophyll a, B5 is a mixed site of chlorophylls a and b in minor complexes (CP29, CP26, and CP24) (*21*). Therefore, a delocalized chlorophyll a dimer can form within the A5 and B5 sites in CP29. Moreover, this dimer structure could also explain why Z^{+} formation is not favored in LHCII (*14*), in which the A5 and B5 sites specifically bind chlorophylls a and b, respectively (*12*). Because the large spectral absorbance gap (~700 cm^{-1}) between chlorophylls a and b prohibits delocalization over a chlorophyll heterodimer, no CT state can be produced in the L2 site of LHCII. One additional factor of specificity is that the capacity of LHCII to undergo exchange of V to Z in site L2 in vivo is very low relative to minor complexes (*22*).
27. X.-P. Li *et al.*, *J. Biol. Chem.* **279**, 22866 (2004).
28. G. Bonente *et al.*, *J. Biol. Chem.* **283**, 8434 (2008).
29. E. Teardo *et al.*, *Biochim. Biophys. Acta* **1767**, 703 (2007).
30. We thank D. Zigmantas for helpful discussions. Supported by Korea Research Foundation grant KRF-2006-214-C00037 funded by the Korean Government (T.K.A.); USDA National Research Initiative competitive grant 2006-03279 (T.J.A.); Office of Basic Energy Sciences, Chemical Sciences Division, U.S. Department of Energy contract DE-AC03-76SF000098 (G.R.F. and K.K.N.); and Italian Basic Research Foundation contract RBLA0345SF and Trento Research Council contract SAMBA (R.B.).

Supporting Online Material
www.sciencemag.org/cgi/content/full/320/5877/794/DC1
Materials and Methods
Figs. S1 to S6
Tables S1 and S2
References

3 January 2008; accepted 7 April 2008
10.1126/science.1154800

Phosphorylation of Retinoblastoma Protein by Viral Protein with Cyclin-Dependent Kinase Function

Adam J. Hume,[1] Jonathan S. Finkel,[2] Jeremy P. Kamil,[3] Donald M. Coen,[3] Michael R. Culbertson,[2] Robert F. Kalejta[1]*

As obligate intracellular parasites, viruses expertly modify cellular processes to facilitate their replication and spread, often by encoding genes that mimic the functions of cellular proteins while lacking regulatory features that modify their activity. We show that the human cytomegalovirus UL97 protein has activities similar to cellular cyclin–cyclin-dependent kinase (CDK) complexes. UL97 phosphorylated and inactivated the retinoblastoma tumor suppressor, stimulated cell cycle progression in mammalian cells, and rescued proliferation of *Saccharomyces cerevisiae* lacking CDK activity. UL97 is not inhibited by the CDK inhibitor p21 and lacks amino acid residues conserved in the CDKs that permit the attenuation of kinase activity. Thus, UL97 represents a functional ortholog of cellular CDKs that is immune from normal CDK control mechanisms.

Cyclin–cyclin-dependent kinase (CDK) complexes are found in all eukaryotes and control cell cycle progression and other processes (*1*). In higher eukaryotes, a major target of the CDKs is the retinoblastoma (Rb) tumor-suppressor protein that controls progression through G_1 phase of the cell cycle. The pathway controlled by Rb may be aberrant in most human cancers (*2*). Unphosphorylated Rb binds to E2F transcription factors, thus inhibiting the expression of genes required for DNA replication and arresting cell cycle progression in G_0 or G_1 phase. During normal cell cycle progression, Rb is functionally inactivated by multiple phosphorylations mediated sequentially by a series of CDK complexes (*3*). Phosphorylation of Rb disrupts complexes with E2Fs, allowing for cell cycle progression into S phase. To create an advantageous cellular environment for viral replication, viruses can inactivate Rb through direct binding of viral proteins to Rb and the consequent disruption of Rb-E2F complexes, by causing Rb degradation, or through constitutive activation of cellular CDKs by virally encoded cyclin proteins (*4*, *5*). Here, we describe a virally encoded protein kinase that directly phosphorylates Rb, and we show that this kinase can substitute for CDKs during cell cycle regulation.

Upon infection of quiescent cells with human cytomegalovirus (HCMV), unphosphorylated Rb is first degraded by pp71 (*6*) and then phosphorylated (*7*, *8*) (Fig. 1A and fig. S1). Phosphorylated Rb migrates more slowly during SDS–polyacrylamide gel electrophoresis than does the unphosphorylated form of the protein, and it can be detected in lysates from HCMV-infected cells within 4 hours after infection (Fig. 1A). Three small-molecule inhibitors of CDK activity (roscovitine, olomoucine, and flavopiridol) inhibited Rb phosphorylation induced by serum stimulation, but not phosphorylation induced by HCMV infection (Fig. 1B). Additional experiments with a panel of 20 kinase inhibitors (table S1) revealed that only 2, Gö6976 and NGIC-I, inhibited Rb phosphorylation during HCMV infection (Fig. 1C). These drugs inhibit both cellular protein kinase C (PKC) and the HCMV protein kinase UL97 (*9*). However, Gö7478, an inhibitor of PKC that does not inhibit UL97, did not reduce Rb phosphorylation in HCMV-infected cells (Fig. 1C). Because an HCMV mutant lacking the UL97 gene (*10*) did not induce Rb phosphorylation (Fig. 1, D and E) and because of the presence of three potential Rb-binding motifs in UL97 (fig. S2), we suspected that UL97 was required for Rb phosphorylation during HCMV infection.

Phosphorylation of Rb on Ser^{780}, Ser^{807}, Ser^{811}, and Thr^{821} inactivates the cell cycle–inhibitory and tumor-suppressor functions of Rb by disrupting Rb-E2F complexes (*3*). All of these residues are phosphorylated in HCMV-infected cells (Fig. 2A). Residues not known to modify Rb function upon phosphorylation, such as Ser^{249} and Thr^{252}, were not phosphorylated in HCMV-infected cells but were phosphorylated in serum-stimulated cells (Fig. 2A). A recombinant HCMV in which the wild-type (WT) UL97 gene was replaced with an allele encoding a UL97 protein substituted at the active site Lys (Lys^{355} → Gln^{355}; K355Q) failed to induce phosphorylation of Rb, but a WT revertant virus derived from the K355Q mutant did induce the phosphorylation of Rb (Fig. 2B). The UL97-K355Q mutant virus exhibited a growth defect similar to that of the UL97-null virus, and the growth defect was rescued in the revertant virus (fig. S3). The CDK inhibitor flavopiridol again failed to prevent HCMV-induced phosphorylation of Rb in HCMV-infected cells, but two drugs that inhibit UL97 kinase activity (Gö6976 and maribavir) did inhibit such phosphorylation (fig. S4). Thus, in HCMV-infected cells, kinase activity of UL97 is necessary for Rb phosphorylation on residues that inactivate its function. Rb degradation and phosphorylation in HCMV-infected cells are independent events (fig. S1).

We also tested whether UL97 alone is sufficient to induce Rb phosphorylation. Transfection of expression plasmids for epitope-tagged wild type [but not a catalytically inactive (Lys^{355} → Met^{355}; K355M) mutant (*11*)] induced the phosphorylation of cotransfected Rb on inactivating residues (Fig. 3A) in Saos-2 cells that are intrinsically unable to phosphorylate Rb. Drugs that inhibit UL97 partially suppressed Rb phosphorylation when added to UL97-expressing

[1]Institute for Molecular Virology and McArdle Laboratory for Cancer Research, University of Wisconsin-Madison, Madison, WI 53706, USA. [2]Laboratories of Genetics and Molecular Biology, University of Wisconsin-Madison, Madison, WI 53706, USA. [3]Department of Biological Chemistry and Molecular Pharmacology, Harvard Medical School, Boston, MA 02115, USA.

*To whom correspondence should be addressed. E-mail: rfkalejta@wisc.edu